Astron. Astrophys. 316, 384–395 (1996)

ASTRONOMY AND ASTROPHYSICS

A comparison of interplanetary coronal mass ejections at Ulysses with Yohkoh soft X-ray coronal events

L.A. Weiss[1], J.T. Gosling[1], A.H. McAllister[2], A.J. Hundhausen[2], J.T. Burkepile[2], J.L. Phillips[1], K.T. Strong[3], and R.J. Forsyth[4]

[1] Los Alamos National Laboratory, Los Alamos, NM 87545, USA
[2] High Altitude Observatory / NCAR, Boulder, CO 80307, USA
[3] Lockheed Solar and Astrophysics Laboratory, Palo Alto, CA 94304, USA
[4] Imperial College, Blackett Laboratory, London, SW7 2BZ, UK

Received 9 February 1996 / Accepted 14 March 1996

Abstract. Coronal Mass Ejections (CMEs) observed at several AU by the Ulysses spacecraft are mapped radially back to the Sun and compared with Yohkoh Soft X-ray Telescope (SXT) images of the corona in an effort to identify correlated events. Correlations between the observations were difficult to make during the ecliptic phase of the Ulysses mission when the satellite footprint was at low heliographic latitudes and the Sun was particularly active. During its traversal to high southerly latitudes (February 1992 - September 1994), however, the correspondence became clearer for two reasons: 1) the radial velocity profiles of the high-latitude CMEs were better preserved since they were less likely to be driving shocks or to have interacted with high-speed streams; and 2) solar activity decreased, making it easier to discern individual and/or low-intensity events in the SXT images. We describe five Ulysses-observed CMEs which correlated with spatially and temporally isolated coronal X-ray events in the Yohkoh SXT images, concentrating on similarities and differences between their solar wind and coronal structures. Two of the five events appeared to have been initiated concurrently with active region (AR) flares; the other three involved the restructuring of low-intensity, polar crown arcades. Significantly, however, all five events exhibited an "LDE" signature, though only the two AR events generated a detectable signal above the GOES integrated background X-ray flux. The characteristics of the interplanetary CMEs were not well correlated with their coronal X-ray signatures: similar-looking coronal events produced very different interplanetary field structures, and different-looking coronal signatures evolved into remarkably similar structures at Ulysses. Although we suspect that all of the events may have had an initially helical field structure, only three of the events displayed coherent field rotations characteristic of nearly force-free flux ropes (two of these were associated with polar crown arcades and one with an AR flare). It appears that the most important factor in determining the magnetic field evolution of a CME in interplanetary space is its plasma beta, but that it is very difficult to predict the interplanetary beta based on the post-eruption coronal X-ray signature.

Key words: Sun: corona – solar wind – Sun: magnetic fields – plasmas

Send offprint requests to: L.A. Weiss

1. Introduction

Coronal mass ejections (CMEs) involve the expulsion of substantial quantities ($10^{15} - 10^{16}$g) of solar material outward into interplanetary space. The ejected plasma drags a portion of the solar magnetic field with it, resulting in the restructuring of the near-coronal magnetic field and the formation of closed magnetic field structures extending far out into the solar wind. CME-driven interplanetary disturbances are now known to be the cause of virtually all large, non-recurrent geomagnetic storms (e.g., Gosling et al. 1991; Kahler 1992; Webb 1992). Approximately 1/3 of the CMEs identified in the solar wind near Earth exhibit large-scale field rotations characteristic of nearly force-free magnetic flux ropes (Gosling, 1990); this helical topology is believed to be a natural consequence of 3-dimensional reconnection of the coronal field lines behind the departing CMEs (Gosling 1993).

In the corona, CMEs can be directly imaged by white-light coronagraphs when they occur within $\sim 35^\circ$ of the solar limb (Hundhausen 1993). CMEs are frequently observed in association with other forms of solar activity, the most common being Hα filament eruptions and long-decay soft X-ray flares (LDEs) (e.g., Munro et al. 1979; Webb & Hundhausen 1987; St. Cyr & Webb 1991; Hundhausen 1996). The LDE emission results from the formation of new magnetic loops low in the corona and is thus believed to be the signature of reconnection behind the outward moving CMEs (e.g., Kopp & Pneuman 1976; Hiei et al. 1993).

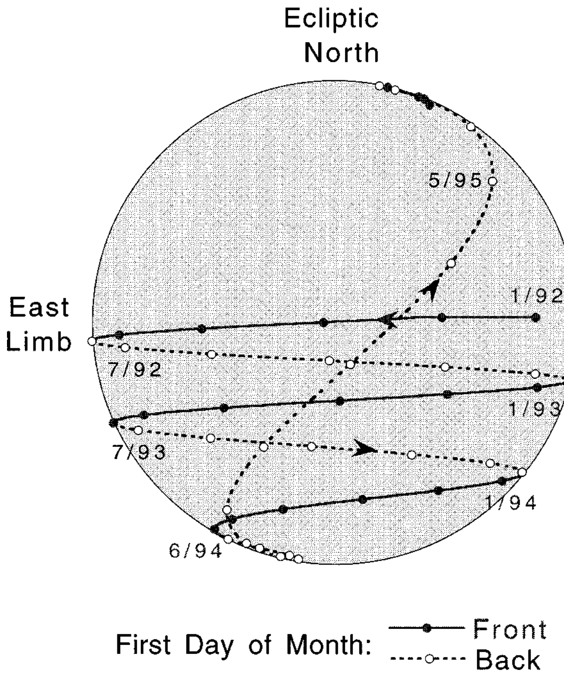

Fig. 1. The orbital trajectory of Ulysses through June, 1995, mapped onto the Sun as seen from Earth.

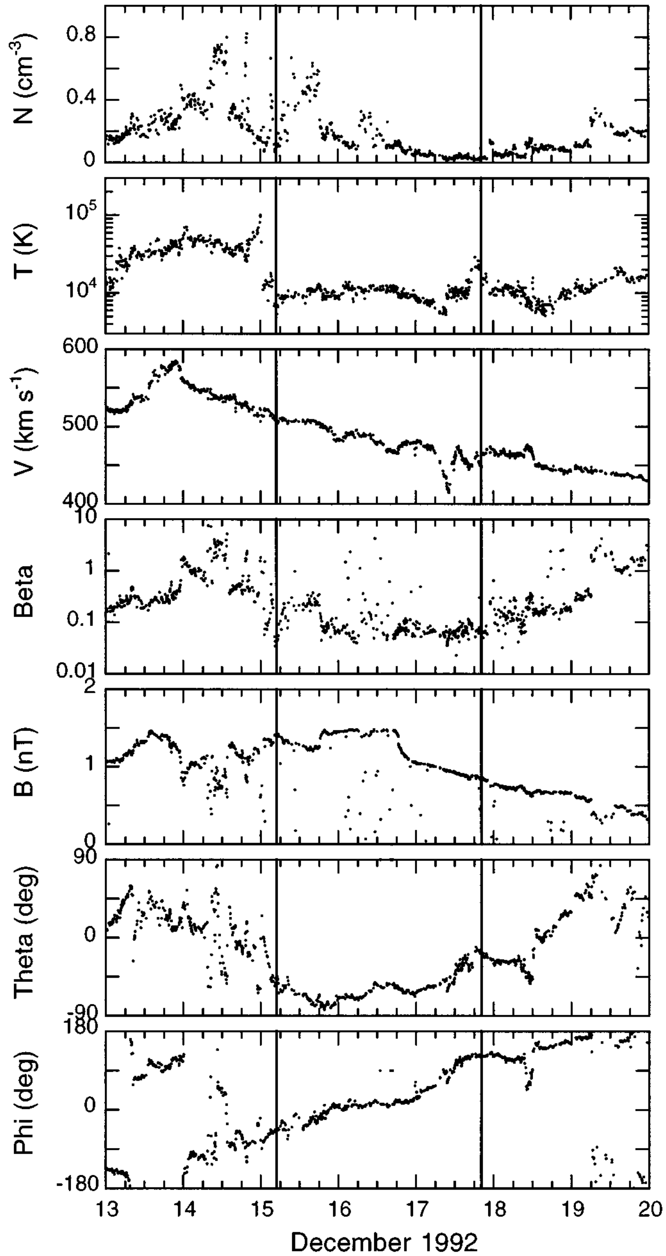

Fig. 2. Selected plasma and magnetic field parameters observed by Ulysses in association with the passage of an interplanetary CME between December 15–17, 1992. Plotted from top to bottom are proton density, proton temperature, bulk flow speed, total plasma beta, magnetic field magnitude, and polar and azimuthal angle of the magnetic field. The interval of bi-directional electron flux is marked with vertical lines.

New opportunities to investigate coronal restructuring in the aftermath of a CME are now available using full disk coronal images from the Soft X-ray Telescope (SXT) on the Yohkoh satellite. Studies of mass ejections near the limb observed simultaneously by coronagraphs and the SXT show that at least some CMEs involve the expansion, eruption, and subsequent reformation of coronal X-ray arcades and white light streamers (Hiei et al. 1993; Sime et al. 1994; Hundhausen 1995). CMEs do not occur exclusively on the limb, however, and other recent studies, including this one, have begun to examine the X-ray signatures of filament eruptions and/or mass ejections on the solar disk (McAllister et al. 1992; Hanaoka et al. 1994; McAllister et al. 1996). Since mass ejections from the center of the disk are the ones most likely to intercept Earth, identification of their X-ray aftermath signatures represents a significant forecasting ability.

In this paper we present observations of interplanetary CMEs observed by Ulysses and what we believe to be the Yohkoh SXT signatures associated with their ejection. This comparison allows us to study the post-ejection X-ray signatures of different CMEs and to examine the relationship between those signatures and the interplanetary characteristics of the CMEs.

2. Experimental approach

Our search for mass ejections observed by both Yohkoh and Ulysses was limited to events observed between November and June, 1991-1992, 1992-1993, and 1993-1994. As Fig. 1 shows, these are the periods during which the Ulysses spacecraft trajectory mapped to the Earthward side of the solar disk. For each of the CMEs encountered by Ulysses during these intervals the ejection date was estimated using the measured speed of the CME, and then Yohkoh and other ground-based observations were examined for evidence of the corresponding ejection. These steps, including the assumptions and potential problems associated with each, are described below.

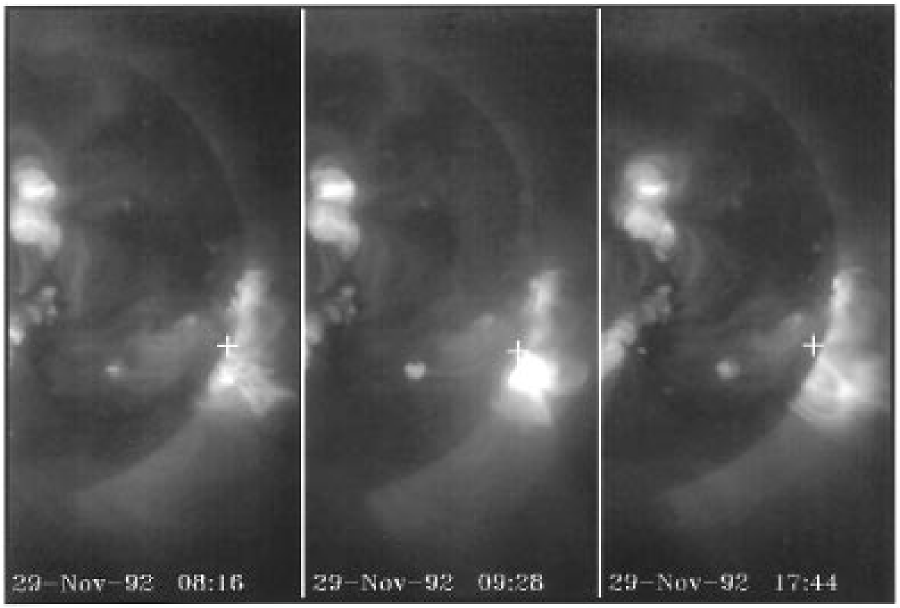

Fig. 3. Yohkoh SXT images showing the development of the AR flare and post-flare loops believed to be associated with the interplanetary CME observed by Ulysses on December 15–17, 1992. The position of the Ulysses footpoint is marked by a cross.

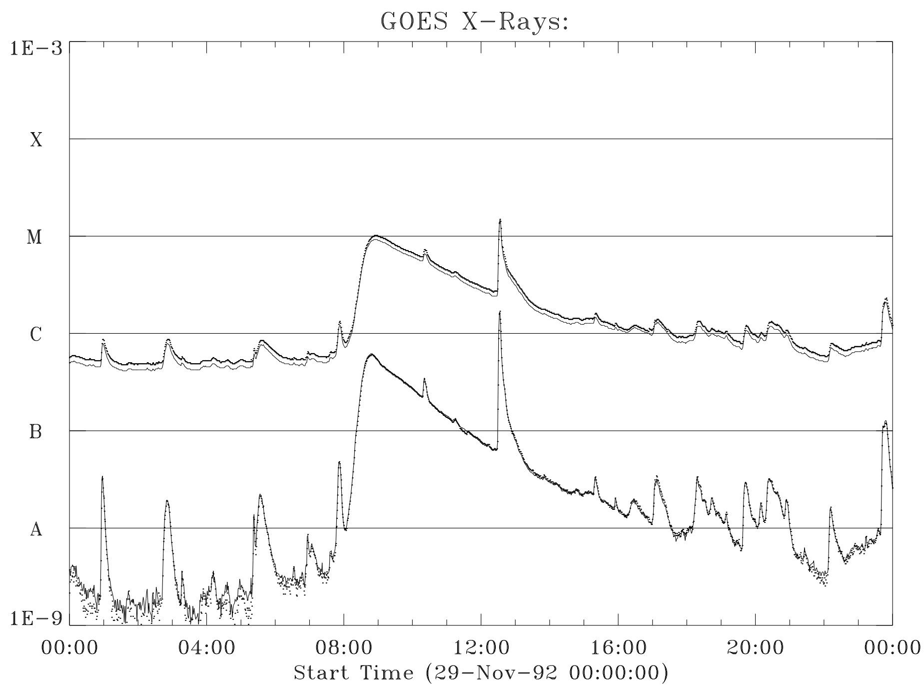

Fig. 4. Full-sun integrated x-ray fluxes (W/m^2) measured by the GOES satellite on November 29, 1992. The upper traces are from the 1 - 8 Å wavelength band and the lower from the 0.5 - 4 Å band.

2.1. Identification of CMEs in Ulysses plasma and field data

The Ulysses payload includes vector helium and fluxgate magnetometers for interplanetary magnetic field measurements (Balogh et al. 1992) and a Los Alamos solar wind plasma analyzer for the measurement of 3-dimensional ion (0.257 - 35.0 keV/charge) and electron (0.81 - 862 eV) distributions (Bame et al. 1992). The initial identification of CMEs in the solar wind plasma data was based on a bi-directional heat flux in the 2-dimensional (energy - azimuth) electron distributions. Bi-directional streaming of suprathermal electrons is expected if both ends of an interplanetary magnetic field line are rooted in the hot corona (e.g., Gosling et al. 1987, 1992). This feature is readily apparent in energy-azimuth spectrograms as field-aligned enhancements at angles separated by 180°. A bi-directional heat flux may also result from magnetic connection between an upstream spacecraft and a planetary or corotating shock (Gosling et al. 1993a). For this study, counterstreaming electron events associated with connections to the Jupiter bow shock (Moldwin et al. 1993) and to forward and reverse shocks associated with corotating interaction regions (CIRs) were eliminated from consideration.

In addition to the presence of counterstreaming suprathermal electrons, a number of other anomalous plasma and field characteristics are commonly associated with CMEs in the so-

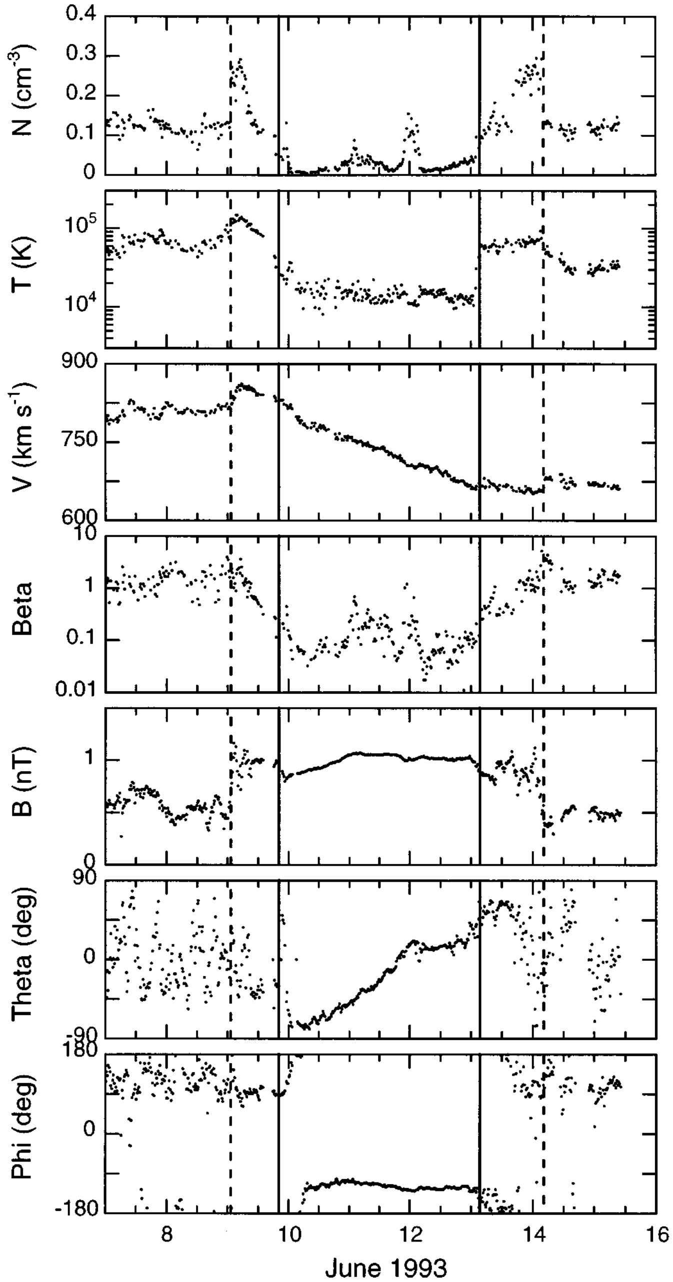

Fig. 5. Plasma and magnetic field parameters observed by Ulysses for the CME encountered between June 10-12, 1993. The format is the same as Fig. 2. The vertical dashed lines denote forward and reverse shocks driven by over-expansion of the CME.

lar wind (e.g., Gosling 1990, 1992). These include: 1) helium abundance enhancements ($He^{++}/H^{+} \gtrsim 0.08$); 2) ion and electron temperature depressions; 3) strong magnetic fields ($\gtrsim$ 8 nT at 1 AU); 4) low plasma beta (< 1.0); 5) low magnetic field strength variance; 6) distinct magnetic field rotations (magnetic clouds or flux ropes); 7) counterstreaming energetic protons ($\gtrsim$ 20 keV); and 8) unusual plasma ionization states (e.g., Fe^{+16}, He^{+}). Fast CMEs having outward speeds sufficiently greater than the ambient solar wind ahead will drive shock waves, which can be also used as an identifying feature. Few of the CMEs identified on the basis of bi-directional electron streaming exhibited all of these secondary characteristics; however, if not even a single secondary characteristic could be identified during the bi-directional streaming interval, the event was eliminated from the study.

2.2. Calculation of the CME ejection date

CMEs are ejected from the Sun with a wide range of outward speeds (Gosling et al. 1976; Howard et al. 1985; Hundhausen et al. 1994). The average speed of in-ecliptic CMEs near 1 AU is comparable to the average speed of the solar wind ($\sim$470 km/s) near Earth (e.g., Gosling et al. 1987). Interplanetary CMEs observed at high heliographic latitudes have higher speeds (average $\sim$730 km/s), comparable to that of the rest of the wind at high latitudes (Gosling 1994). Like the normal solar wind, the ejected plasma moves nearly radially outward from the sun while the magnetic field embedded within the CME is wrapped into the Parker spiral. CMEs that have speeds considerably greater than the preceding solar wind generate shock disturbances as the high-speed ejecta overtakes and interacts with the slow solar wind ahead. In this case, momentum is transferred to the solar wind and the CME is decelerated. It is also possible that CMEs ejected at speeds comparable to or less than the ambient solar wind may be overtaken and accelerated by a high-speed solar wind stream. In both of these cases it is difficult to predict accurately the ejection date of the CME since a knowledge of its outward velocity profile is required for the calculation.

The most confident prediction of ejection date is for CMEs which leave the Sun at speeds comparable to or less than the ambient solar wind ahead and which have not been "swept up" by a fast-moving stream. The centers of these CMEs presumably maintain a nearly constant outward speed; thus, they generally have flat or declining speed profiles at Ulysses. Some CMEs accelerate up through the corona, but this effect lowers the average transit speeds of CMEs at several AU by only a few 10's of km/s. Although it is possible with some assumptions to predict the ejection date for CMEs which have decelerated or accelerated in interplanetary space, we will restrict the events discussed in this paper to those with the highest-confidence ejection date calculations (i.e., "coasting" CMEs).

2.3. Survey of the Yohkoh SXT data

The SXT produces high-resolution images of the solar corona at wavelengths corresponding to plasma temperatures between 2×10^{6} and 10^{7} K (Tsuneta et al. 1991). Owing to a combination of higher plasma densities and temperatures, active regions, flares, and some magnetic loops appear bright in these images. For each CME that appeared to be coasting, the position of the Ulysses spacecraft was projected radially back to the Sun and plotted on the SXT images. The images were examined for potentially correlated X-ray events over a $\pm$12 hour window centered on the estimated ejection date and time. A temporal window of this size accounts for inaccuracy in the average outward speed of up

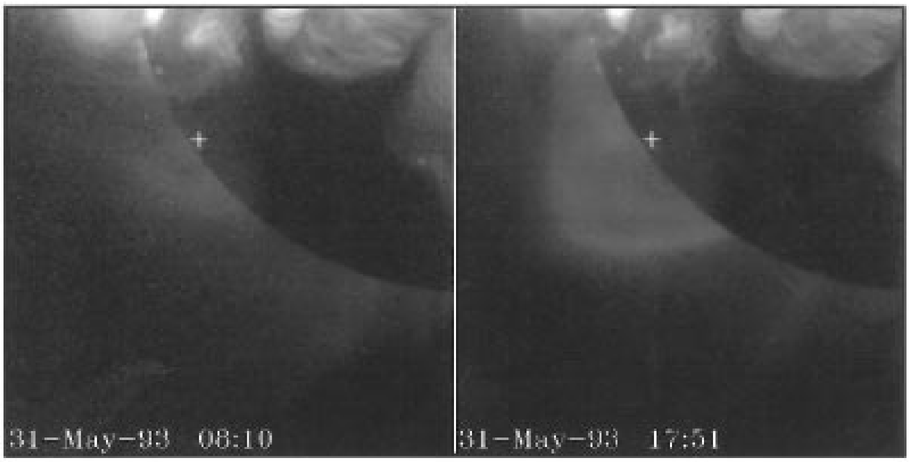

Fig. 6. Yohkoh SXT images showing the development of large coronal loops directly under the radial projection of the Ulysses spacecraft near the predicted launch time of the CME.

to ±15 km/s at $\sim$5 AU and up to ±40 km/s at 3.5 AU. Based on the average extent of ejecta at 1 AU (Richardson & Cane 1993), the spatial window for an associated event was chosen to be a circle of 50° radius centered on the Ulysses footpoint.

We have concentrated on CMEs which coincided with the most temporally and spatially isolated soft X-ray coronal events. This criterion was easier to achieve during the first high-latitude phase of the Ulysses mission (February 1992 - September 1994) as the Ulysses footpoint moved farther away from the active-region belt and as overall solar activity decreased. The most common signature affiliated with the mapped projection of the CMEs was the appearance of a newly-formed arcade of loops, most often of substantial size and fairly low intensity. If the Kopp & Pneuman reconnection scenario is correct, the soft X-ray signature of an ejection should indeed appear as an expanding, cusp-like arcade of loops (Hiei et al. 1993; Sime et al. 1994; Hundhausen 1995). In other cases the SXT images showed a more intense, spatially-limited flare associated with an active region. These flares were also eruptive in nature and showed the formation of new loops, although at a smaller scale. This type of eruptive active region LDE flare is often associated with CMEs. It is important to remember, however, that flares often occur in the absence of CMEs and are generally neither the cause of CMEs nor are centered underneath them (e.g., Kahler et al. 1989; Harrison et al. 1990; Hundhausen 1996).

2.4. Other evidence of the ejection

Other solar activity data were checked for each event of interest. These data included: Mauna Loa coronagraph images (for spatial windows encompassing the solar limb); ground-based Hα images (for eruptive prominences or disappearing filaments); and GOES disk-integrated soft X-ray fluxes (for flare identification and LDE signatures).

3. Observations

In this section we present Ulysses plasma and field data and Yohkoh soft X-ray coronal images for 5 of the most convincing solar wind - solar coronal CME correlations. These events are labeled by the date of the coronal event: November 29, 1992, May 31, 1993, February 1, 1994, February 20, 1994, and April 14, 1994. All of the CMEs except November 29, 1992 were encountered when Ulysses was at heliographic latitudes $\gtrsim 30°$ S (the latitude roughly corresponding to the tilt of the streamer belt at that time). Similarities and differences between these events will be discussed in Sect. 4.

3.1. Event 1: November 29, 1992

Strong counterstreaming suprathermal electrons were observed at Ulysses between 0500 UT on December 15, 1992 and 2030 UT on December 17, 1992. The spacecraft was 5.1 AU from the Sun, at a heliographic latitude of 21.8° S and approximately 12.5° in front of the west solar limb as viewed from Earth. The interval over which the electron distribution peaked at angles separated by 180° is indicated by vertical lines in the ion moment and magnetic field plots shown in Fig. 2. This CME had a somewhat depressed proton temperature, high magnetic field strength with low variance, and a declining speed profile. The azimuthal component of the field (phi) showed a distinct rotation (characteristic of a nearly force-free magnetic flux rope), and the plasma beta within the event was low, generally ≤ 0.1.

Since the CME was neither moving faster than the solar wind ahead of it nor being overtaken by higher- speed solar wind from behind, it is reasonable to assume that its center traveled outward from the Sun at a nearly constant speed. Using a central velocity of 500 km/s, the CME would have left the Sun near the end of the day ($\sim$2200 UT) on November 28. Solar activity was high throughout November 28-29, with a large, equatorial active region traversing the western limb. It seems likely that the origin of the CME was affiliated with this AR. One particular long-duration flare within the AR was highly suggestive of an eruption with trailing reconnection. Although it did not appear off the western limb until nearly 10 hours after the estimated time of the mass ejection, it is possible that the average transit speed was slightly higher than we have assumed.

Fig. 3 shows three SXT images of the western limb on November 29. The first panel shows closed magnetic loops low in the corona which brightened in the 10 min preceding the

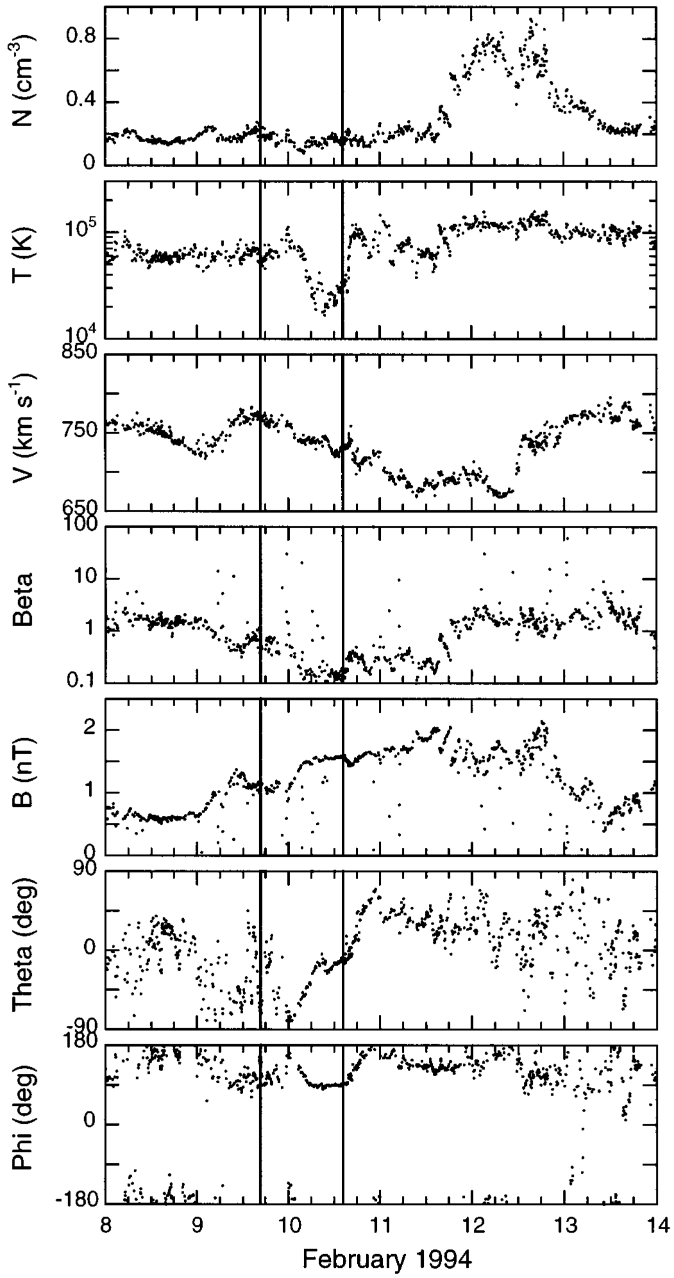

Fig. 7. Plasma and magnetic field parameters observed by Ulysses for the CME encountered between February 9-10, 1994.

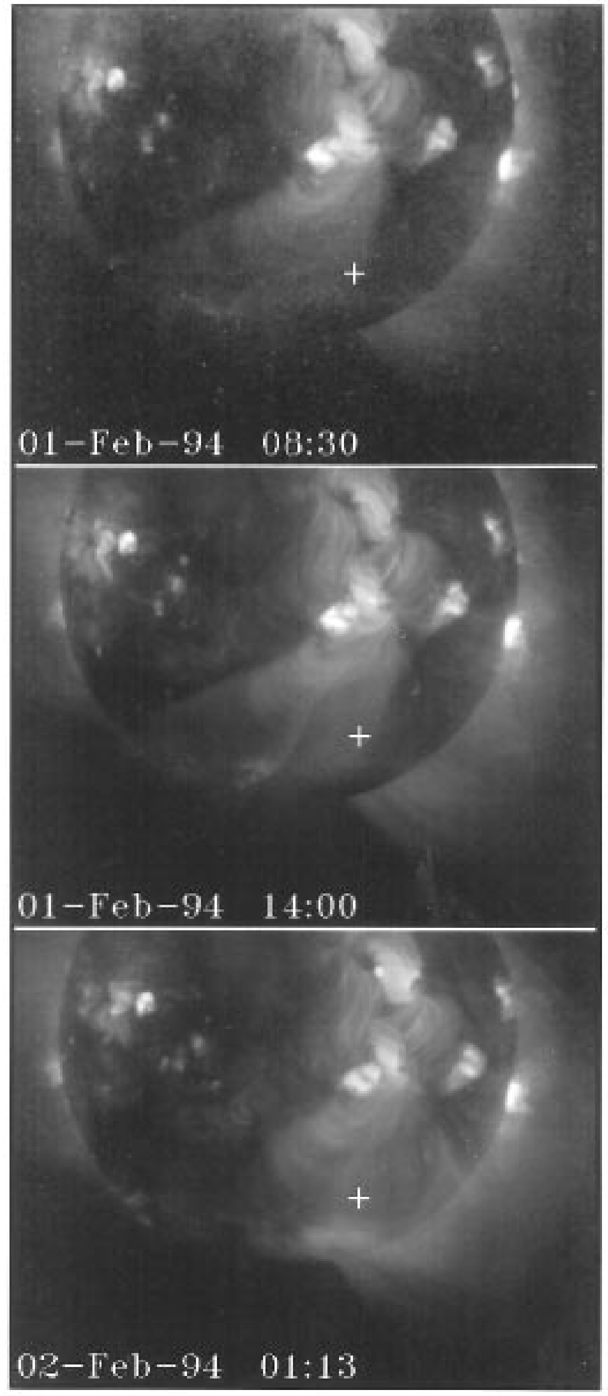

Fig. 8. The restructuring of a large polar arcade associated with the mass ejection shown in Fig. 7. The predicted ejection time for the CME based on its speed at Ulysses was ~1500 UT on February 1, 1994.

image. The region above the loops expanded rapidly outward during this time. The second panel shows the peak of the X-ray flare at ~0930 UT. The third panel, approximately 8 h later, shows the outward progression of the magnetic loops and the expansion of the inner, dark cavity. The GOES soft X-ray data for November 29, 1992 is shown in Fig. 4. The flux in the 1-8 Å band rose above its $\sim 10^{-6}$ W/m^2 background level to a peak value of 10^{-5} W/m^2 just after 0830 UT, then decayed very slowly over the next 12 h. This is the classic LDE signature commonly associated with prominence eruptions and mass ejections (e.g., Hundhausen 1996). Rising, "post-ejection" loops were visible in the SXT images throughout the duration of the LDE. The short-duration peak superimposed on the LDE envelope at ~1230 UT was caused by a flare near the center of the solar disk. Although a number of Hα filaments passed behind the western limb on November 28-29, there was no obvious disk eruption associated with the LDE flare. Mauna Loa coronagraph images were unavailable on November 28 and 29 due to cloud cover; however,

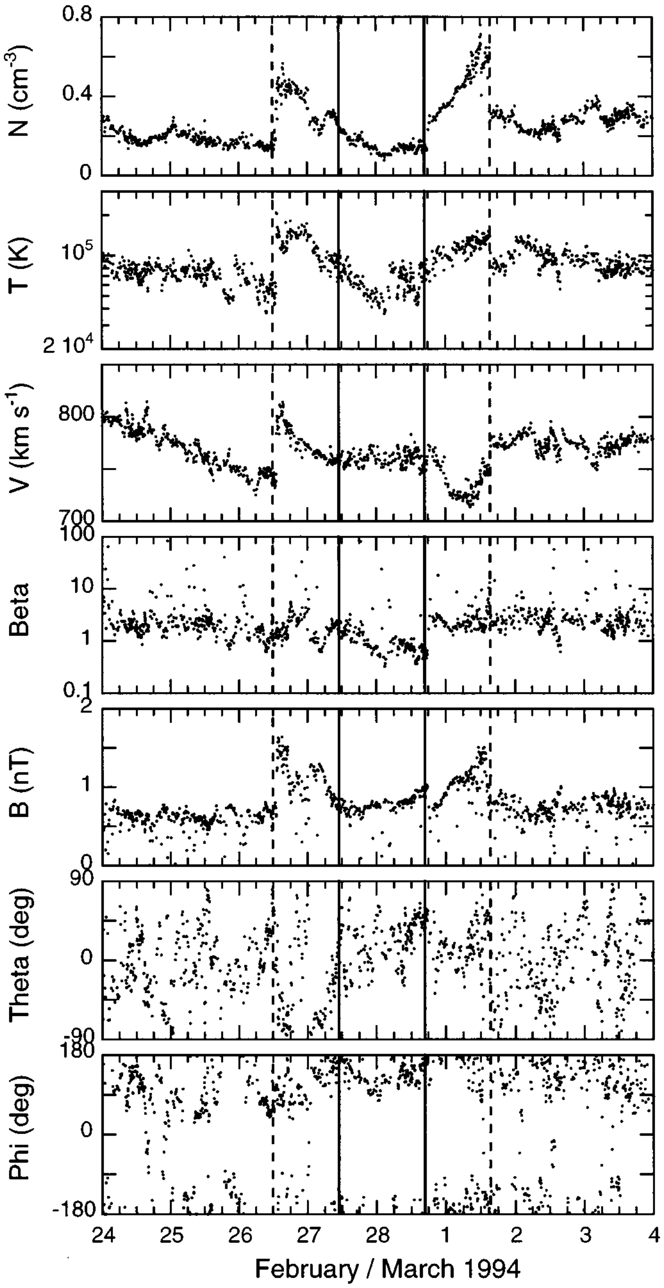

Fig. 9. Plasma and magnetic field parameters observed by Ulysses for the CME encountered between February 27-28, 1994.

the existence of a helmet streamer over the SW limb on the 30th (not visible on the 27th) is at least consistent with the streamer structure expected after a mass ejection (Hundhausen 1995).

3.2. Event 2: May 31, 1993

In this event an interval of counter-streaming electrons encountered by Ulysses between June 9 - 13, 1993, mapped back to within 2 hours of the formation of a large, rising arcade of loops off the SE limb of the Sun on May 31, 1993 (Gosling et al.1994a). Ulysses was located slightly behind the east limb (as viewed from Earth) at a latitude of S32.5° and a distance of 4.6 AU. Fig. 5 shows selected Ulysses solar wind plasma and magnetic field parameters in the same format as Fig. 2. This was the first CME encountered by Ulysses in which a nearly symmetric pair of forward and reverse shocks were observed on either side of the CME (Gosling et al. 1994a,b). Since the shocks were apparently driven by the over- expansion of the CME rather than a velocity differential, we assumed it also maintained a nearly constant outward speed.

This event was distinguished by very low proton density and temperature, a high but declining flow speed ($\sim$750 km/s), and a relatively strong magnetic field of low variance. The polar magnetic field angle showed a very smooth rotation, indicating a flux rope geometry, and the plasma beta within the CME was very low, $\sim$0.1. The development of large coronal loops off the SE limb between 0810 and 1771 UT is documented in the soft X-ray images shown in Fig. 6. There was no distinct elevation of the GOES x- ray flux above the background of $\sim 8 \times 10^{-7}$ W/m^2, nor was there an observed prominence eruption associated with the event. However, the Mauna Loa coronagraph clearly showed a bright, compact helmet streamer over the SE limb on June 1 where none existed on May 30th (no images were available on May 31).

3.3. Event 3: February 1, 1994

Another fast interplanetary CME passed Ulysses between February 9-10, 1994. The spacecraft was 3.62 AU from the Sun, at S52.3° heliographic latitude and $\sim$29° W of Earth, placing its footpoint in the SW quadrant of the solar disk (see Fig. 1). The ion moments and magnetic field components for this event are shown in Fig. 7.

The latter portion of the CME had a depressed ion temperature and the plasma beta was low ($\sim$0.1). The polar angle of the magnetic field (theta) showed a smooth rotation characteristic of a magnetic cloud. It is possible, primarily based on the high field strength and low beta, that Ulysses's encounter with the ejecta actually lasted until midday on February 11; the absence of counterstreaming electrons during this latter interval could be explained by the presence of open field lines within the overall structure of the CME (Gosling et al. 1995a). The center of the CME had a velocity of 740 km/s and if our assumption of nearly constant outward speed is correct, the CME should have left the Sun at about $\sim$1500 UT on February 1, 1994. However, if the radial extent of the CME is indeed larger, its estimated launch time could be as much as 4 h earlier due to its lower central velocity.

Fig. 8 shows a sequence of three images of the southern hemisphere of the Sun on February 1-2, 1994. The coronal event we believe to be affiliated with the departure of the CME consists of the restructuring of a large, previously stable arcade over a mid-latitude extension of the polar crown neutral line. The first panel shows the pre-event coronal arcade running SE from a central active region. Some initial activity occurred along the western edge of the arcade at $\sim$0500 UT, followed by the main phase of the disruption at $\sim$1300 UT. By 0100 UT on February

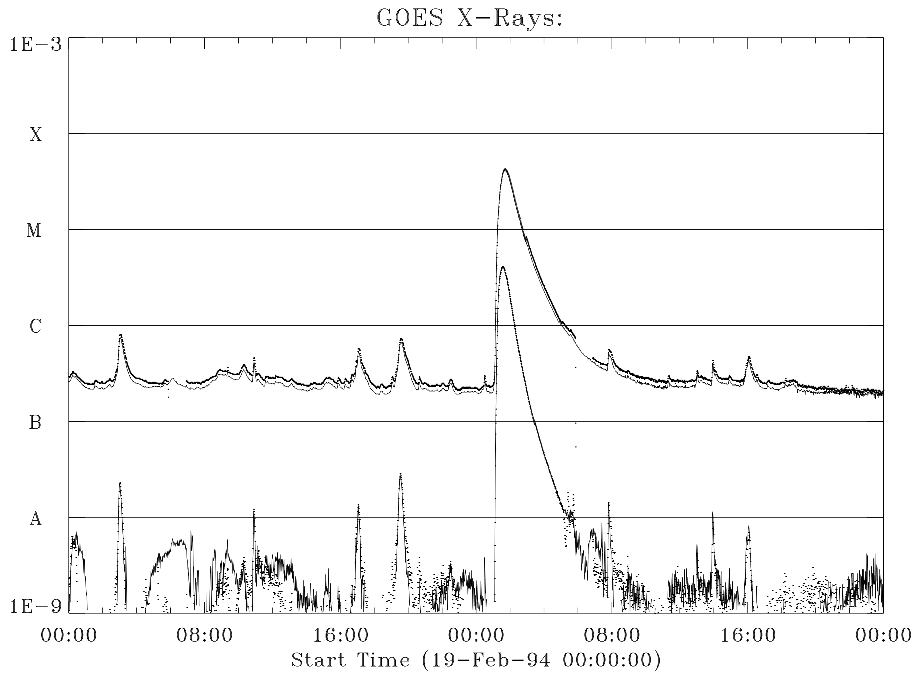

Fig. 10. GOES integrated x-ray fluxes for February 20, 1994, showing the LDE associated with the AR flare in Fig. 11.

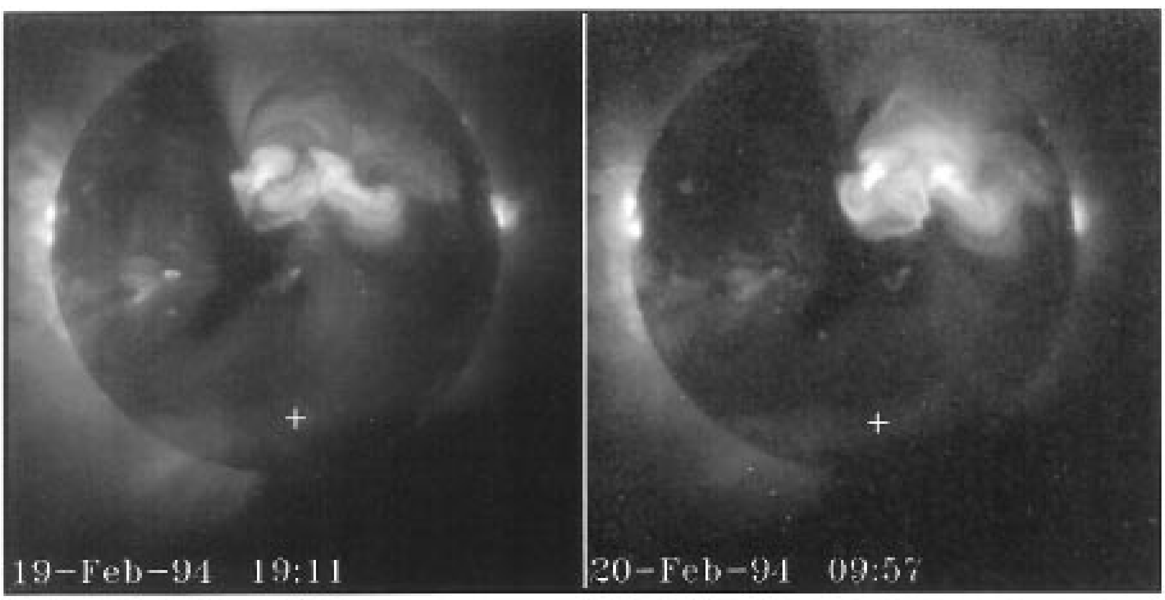

Fig. 11. Yohkoh SXT images of the AR flare on February 19-20, 1994, associated with a CME intercepted by Ulysses on February 27-28.

2, the SE portion of the arcade disappeared and new cusp-like loops appeared off the SW limb. The darkening (opening) of previously bright (closed) field lines is highly suggestive of the eruption of coronal material. The intensity of the arcade's X-ray flux was below the background from the remainder of the Sun ($\sim 1 \times 10^7$ W/m^2), though if one were to integrate the soft X-ray flux at southern latitudes over the 12-17 h course of the event, it would almost certainly have the characteristic LDE shape. Although there were both large and small filaments near the SW limb on February 1-2, there was no obvious evidence of a filament eruption.

3.4. Event 4: February 20, 1994

In this event Ulysses encountered intermittently counterstreaming electrons between 1100 UT on February 27 and 1700 UT on February 28, 1994. At the time of the observations the spacecraft was 3.5 AU from the Sun, at a heliographic latitude of S54.3° and $\sim$11° west of Earth. This was the second CME observed that was bounded by a nearly symmetric forward and reverse shock pair. As is typical for those events, the density, temperature, and field strength peaked just downstream from the shocks and reached minima within the center of the CME (Fig. 9). Compared to the previous events, the plasma beta was

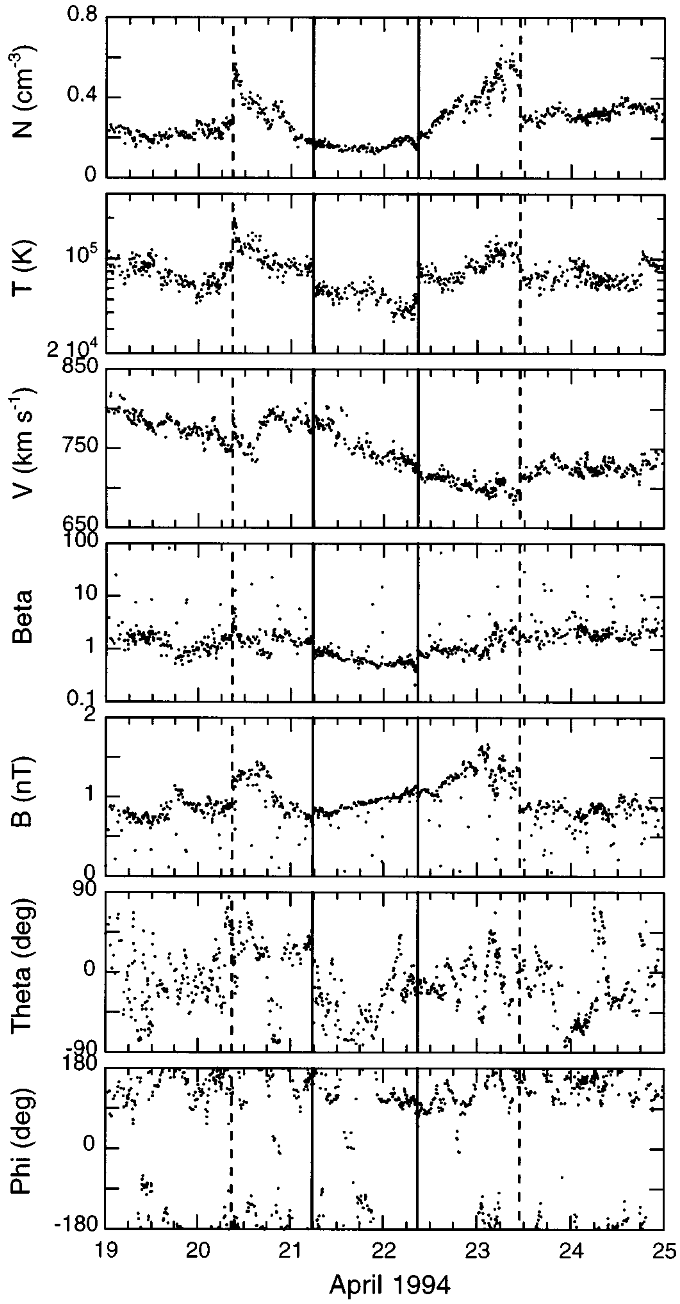

Fig. 12. Plasma and magnetic field parameters associated with the large, polar crown arcade event of April 14, 1994.

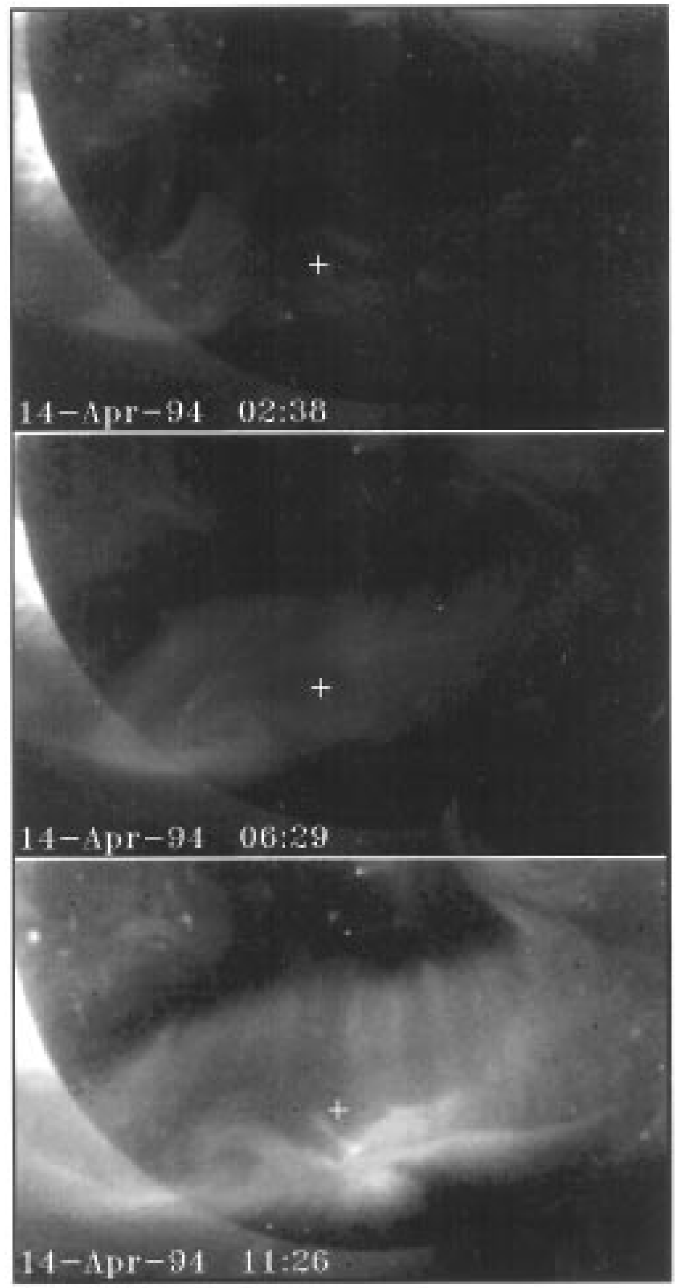

Fig. 13. Dramatic development of a large, polar crown arcade on April 14, 1994.

relatively high ($\sim$ 1.0) and neither component of the magnetic field showed the large-scale rotation characteristic of magnetic clouds. This CME was also observed at low heliographic latitudes by IMP 8 (Gosling et al. 1995b) and was associated with a major geomagnetic storm with a sudden commencement at 0901 on February 21.

Again assuming nearly constant outward speed, the inferred launch time of the CME was $\sim$0100 UT on February 20, in near coincidence with a large, AR flare near the terrestrial subsolar point. Hα images reveal that a large filament on the southern side of the AR erupted (disappeared) as part of this event, which began at 0104 UT and peaked at 0141 UT. GOES soft X-ray emission, shown in Fig. 10, was still well above background more than 8 hours after flare maximum. The first available SXT images of the LDE flare were nearly 8 hours after the flare maximum; the images in Fig. 11 show the pre-eruption (1911 UT, February 19) and post-eruption (0957 UT, February 20) states. Although the flare actually occurred outside the nominal 50° association window, the high degree of timing and lack of other visible X-ray events lend confidence to the correlation. Since coronal magnetic field lines are known to extend well beyond their active-region footpoints, it is probable that the CME was not centered above the flare, but rather was ejected over a much larger region. Synoptic maps of the white-light streamers and coronal magnetic field polarity indicate that the flare may have been located along the global neutral line; this interpretation is consistent with the fact that the azimuth angle of the interplanetary magnetic field in the vicinity of the CME (Fig. 9) had an inward polarity and did not show a magnetic field reversal, indicating that at least the portion of the event observed by Ulysses occurred south of the heliospheric current sheet.

3.5. Event 5: April 14, 1994

Ulysses encountered an episode of sporadic bi-directional suprathermal electrons between 0545 UT on April 21, 1994, and 0850 UT on April 22, 1994, while at a radial distance of 3.2 AU. The spacecraft's footpoint mapped to S60.6° heliographic latitude and just east of central meridian. This CME, the last encountered by Ulysses in its equator-to-south-pole pass, was over-expanding and driving a nearly symmetric pair of forward and reverse shocks. Its plasma and field parameters (Fig. 12) are remarkably similar to Event 4 with minima in proton density, temperature, and field strength occurring within the CME and maxima in these parameters occurring directly downstream of the shocks. Also like Event 4, the CME did not exhibit the large-scale field rotation characteristic of magnetic clouds. It had a declining speed profile with a central velocity of 750 km/s, putting its estimated ejection at approximately 0830 UT on April 14, 1994.

The soft X-ray coronal event (and geomagnetic storm) associated with this CME was quite dramatic and has been discussed in detail by McAllister et al. (1996) and references therein. Unlike Event 4, the mass ejection signature was not affiliated with an active region, but rather with the development of a large arcade of loops over the southern polar crown neutral line. Fig. 13 shows a sequence of images which outline the development of the event, which began as a cusp-like structure over the SE limb and transformed into a large, westward-expanding arcade. The first image at 0238 UT is the first in which the arcade can be seen. The second image shows the partially developed arcade as it expanded toward the west, and the third image shows the fully developed arcade which spanned solar latitudes from 15° - 60° S and affected an area of ∼150° in longitude.

The inferred ejection time based on the speed of the CME at Ulysses is during the peak of the coronal arcade development, perhaps indicating that the CME underwent some initial acceleration (which would lower its average transit velocity and thus push its estimated ejection time back by a few hours), or that the portion of the ejecta which intercepted Ulysses departed later than the easternmost portion of the CME. The speed of the CME at 60° S (∼750 km/s) and in the ecliptic plane (∼570 km/s, inferred from the start of the geomagnetic storm at Earth) implies that this CME most likely underwent an asymmetric evolution in the meridional plane (e.g., Hammond et al. 1995; McAllister et al. 1996).

Table 1. Coronal and interplanetary features of Ulysses/Yohkoh CMEs.

coronal / interplanetary feature	Event 1	2	3	4	5
AR	√			√	
polar arcade		√	√		√
LDE	√	√	√	√	√
flux rope	√	√	√		
low beta	√	√	√		
over-expansion		√		√	√

4. Discussion and summary

We believe that it is possible, under favorable circumstances, to associate with high confidence the observation of a CME in the solar wind with the soft X-ray signature of the coronal restructuring behind the CME. "Favorable circumstances" include an unencumbered path of the ejected material from the corona out to Ulysses (the ejecta is neither accelerated nor decelerated), temporally and spatially isolated soft X-ray coronal events near the predicted ejection time, and whenever possible, corroborating evidence such as coronagraph or Hα images of the coronal event. The five Ulysses - Yohkoh CME correlations presented in this paper are very convincing in these respects, especially with regard to the uniqueness of the X-ray events within the temporal and spatial association windows. We note that the random probability of identifying a coronal X-ray event in a 24 h interval during the November, 1992 - May, 1993 time period (Events 1 and 2) was approximately 0.35; for the three events observed in February - April, 1994, the probability was less than 0.2.

Table 1 summarizes similarities and differences between the coronal and interplanetary observations for the five events. Two of the five events appear to have been initiated concurrently with active region flares; the other three involved the restructuring of low-intensity, polar crown arcades. Studies of mass ejections observed simultaneously near the solar limb by the Mauna Loa Coronagraph and the SXT confirm this duality of coronal ejection signatures (Hundhausen 1995). Significantly, however, all five events exhibited an "LDE" signature, though only the two AR events generated a detectable signal in the GOES integrated X-ray flux. These observations suggest that both 'types' of mass ejections, despite the differences in scale of their X-ray signatures, are affiliated with new loop formation and reconnection of the magnetic field lines behind the CME.

Gosling et al. (1995a) suggest that such trailing reconnection should proceed in three dimensions, thereby producing helical field structures in the solar wind. However, only three of the five CMEs (Events 1, 2, and 3) show the large-scale interplanetary field rotations characteristic of nearly force-free magnetic flux ropes. If the field structure of all the events is initially helical, why do only these three events display coherent internal field rotations? The answer may be related to the plasma beta of the interplanetary CMEs: the three nearly force-free flux-ropes had low plasma beta ($\beta \leq 0.1$) while the other two events had high beta ($\beta \sim 1.0$). Helical structures dominated by the magnetic field should relax into a force-free state as they propagate outward in interplanetary space, while those dominated by plasma pressure should not (Gosling 1996). It seems probable that Events 4 and 5 are helical flux ropes, but not of the force-free variety. The mystery, however, is how some CMEs evolve into high-beta structures if they all originate in magnetically closed, low-beta regions on the Sun.

An alternate explanation for the lack of coherent field rotation in Events 4 and 5 is that Ulysses encountered the edge of a nearly force-free flux rope very similar to Events 1, 2, and 3. If so, the observed high beta and minimal field rotation would be a natural consequence of sampling such a structure close to its edge. However, it is our experience that the transition from high to low beta generally occurs rather rapidly at the edges of force-free flux ropes (e.g., Fig. 5) and thus we are led to believe that the lack of coherent helicity in Events 4 and 5 is most likely not an edge effect, but due to an inherently high beta throughout the structure.

Unlike its relationship with plasma beta, the characteristics of an interplanetary CME do not appear to be well correlated with its coronal X-ray signature. Similar-looking coronal events can produce very different interplanetary field structures (e.g., Event 2 vs. Event 5) and different-looking coronal events can evolve into remarkably similar interplanetary structures (Event 4 vs. Event 5). Events 2 and 5 both exhibited large-scale, low-intensity coronal loop formation, but only (the low-beta) Event 2 evolved into a nearly force-free flux rope. Comparison of Events 4 and 5 (Figs. 11 and 13) shows that the two ejections, one with an AR flare signature and the other with a polar crown arcade signature, had nearly identical plasma and field parameters when they passed the Ulysses spacecraft in February and April, 1994 (Figs. 9 and 12). Both CMEs produced forward / reverse shock pairs as a result of over-expansion, and neither exhibited large-scale field rotations. Both CMEs must also have had sufficient interplanetary latitudinal extent to be observed by Ulysses at $\sim$S55° and to trigger geomagnetic storms at Earth in the ecliptic plane (Gosling et al. 1995b; McAllister et al. 1996).

In conclusion, we have found that while it is possible to associate certain interplanetary CMEs with distinct, post-eruption coronal X-ray signatures, it is very difficult to predict the type of signature based solely on the interplanetary characteristics of the CME, and visa versa. In this sense our findings are similar to that of previous CME - X-ray flare studies, namely that the characteristics CMEs observed in the corona have no apparent relationship to the characteristics (brightness, duration, size, etc.) of CME-associated flares. While it appears that the most important factor in determining the magnetic field evolution of CMEs is their plasma beta, it is unlikely that the interplanetary beta can be determined from images of their post-eruption X-ray signatures.

Acknowledgements. Hα patrol images, archived at HAO, were provided by the Cal Tech Big Bear Observatory and the NOAO Sacrameto Peak Observatory. The first author would like to acknowledge Greg Slater at Lockheed Palo Alto for assistance in the initial analysis of the Yohkoh images, and Pete Riley at Los Alamos National Laboratory for many helpful discussions. The work at LANL was performed under the auspices of the Department of Energy and was supported, in part, by NASA. The Yohkoh satellite is a project of the Institute of Space and Astronautical Sciences of Japan.

References

Bame S.J., McComas D.J., Barraclough D. J., et al., 1992, A&AS 92, 237

Gosling J. T., 1990, in: Physics of Magnetic Flux Ropes, eds. C.T. Russel, E. R. Priest, L. C. Lee, Geophys. Monogr. Ser. 58,. AGU, Washington, D.C., p. 343

Gosling J.T., 1992, in: Eruptive Solar Flares, Lecture Notes in Physics, eds. Z. Svestka, B. V. Jackson, M. E. Machado, Springer-Verlag, New York, p. 258

Gosling J.T., 1993, J. Geophys. Res. 98, 18937

Gosling J.T., 1994, in: Solar Dynamic Phenomena and Solar Wind Consequences, Proc. of the Third SOHO Workshop, ESA Sp-373, p. 275

Gosling J.T., 1996, ARA&A (in press)

Gosling J.T., Hildner E., MacQueen R. M., et al., 1976, Solar Phys. 48, 389

Gosling J.T., Baker D.N., Bame S.J., et al., 1987, J. Geophys. Res. 92, 8519

Gosling J.T., McComas D.J., Phillips J.L., Bame S.J., 1991, J. Geophys. Res. 96, 7831

Gosling J.T., McComas D.J., Phillips J.L., Bame S.J., 1992, J. Geophys. Res. 97, 6531

Gosling J.T., Bame S.J., Feldman W.C., et al., 1993, Geophys. Res. Lett. 20, 2335

Gosling J.T., Bame S.J., McComas D.J., et al., 1994a, Geophys. Res. Lett. 21, 237

Gosling J.T., McComas D.J., Phillips J.L., et al., 1994b, Geophys. Res. Lett. 21, 2271

Gosling J.T., Birn J., Hesse M., 1995a, Geophys. Res. Lett. 22, 869

Gosling J.T., McComas D.J., Phillips J.L., et al., 1995b, Geophys. Res. Lett. 22, 1753

Hammond C.M., Crawford G.K., Gosling J.T., et al., 1995, Geophys. Res. Lett. 22, 1169

Hanaoka Y., et al., 1994, PASJ 46, 205

Harrison R.A., Hildner E., Hundhausen A.J., Sime D.G., Simnett G.M., 1990, J. Geophys. Res. 95, 917

Hiei E., Hundhausen A.J., Sime D.G., 1993, Geophys. Res. Lett. 20, 2785

Howard R., Sheeley N.R., Koomen M.J., Michels D.J., 1985, J. Geophys. Res. 90, 8173

Hundhausen A.J., 1993, J. Geophys. Res. 98, 13177

Hundhausen A.J., 1995, in: Cosmic Winds and the Heliosphere, eds. J. R. Jokipii, C. P. Sonett, M. S. Giampapa, (in press)

Hundhausen A.J., 1996, in: The Many Faces of the Sun., eds. K. Strong, J. Saba, B. Haisch, Springer-Verlag, New York (in press)

Hundhausen A.J., Burkepile J.T., St. Cyr O.C., 1994, J. Geophys. Res. 99, 6543

Kahler S.W., 1992, ARA&A 30, 113

Kahler S.W., Sheeley N.R., Liggett M., 1989, ApJ 344, 1026

Kopp R.A., Pneuman G.W., 1976, Sol. Phys. 50, 85

McAllister A., Uchida Y., Tsuneta S., et al., 1992, PASJ 44, L205

McAllister A., Dryer M., McIntosh P., Singer H., Weiss L., 1996, J. Geophys. Res., 101, 13497

Moldwin M.B., Scime E., Bame S., Gosling J., Phillips, J., Balogh A., 1993, Planet. Space Sci 41, 795
Munro R.H., Gosling J.T., Hildner E., et al., 1979, Sol. Phys. 61, 201
Richardson I.G., Cane H.V., 1993, J. Geophys. Res. 98, 15295
Sime D.G., Hiei E., Hundhausen A.J., 1994, in: X-Ray Solar Physics from Yohkoh, eds. Y. Uchida, T. Watanabe, K. Shibata, H. S. Hudson, Universal Academy Press, Tokyo, p. 197
St.Cyr O.C., Webb D.F., 1991, Sol. Phys. 136, 379
Tsuneta S., Acton L., Bruner M., et al., 1991, in: The Yohkoh (Solar-A) Mission, eds. Z. Svestka, Y Uchida, Kluwer, p. 37
Webb D.F., 1992, in: EruptiveSolar Flares, Lecture Notes in Physics, eds. Z Svestka, B. V. Jackson, M. E. Machado, Springer-Verlag, New York, p. 234
Webb D.F., Hundhausen A.J., 1987, Sol. Phys. 108, 383